Anal. Chem. **2005,** *77,* 585−590

On-Chip Native Gel Electrophoresis-Based Immunoassays for Tetanus Antibody and Toxin

Amy E. Herr,* Daniel J. Throckmorton, Andrew A. Davenport,† and Anup K. Singh

Sandia National Laboratories, Livermore, California 94551

By integrating photopolymerized cross-linked polyacrylamide gels within a microfluidic device, we have developed a microanalytical platform for performing electrophoresis-based immunoassays. The microfluidic immunoassays are performed by gel electrophoretic separation and quantitation of bound and unbound antibody or antigen. To retain biological activity of proteins and maintain intact immune complexes, nondenaturing polyacrylamide gel electrophoresis conditions were investigated. Both direct (noncompetitive) and competitive immunoassay formats are demonstrated in microchips. A direct immunoassay was developed for detection of tetanus antibodies in buffer as well as diluted serum samples. After an off-chip incubation step, the immunoassay was completed in less than 3 min and the sigmoidal dose−response curve spanned an antibody concentration range from 0.17 to 260 nM. The minimum detectable antibody concentration was 0.68 nM. A competitive immunoassay was also developed for tetanus toxin C-fragment by allowing unlabeled and fluorescently labeled tetanus toxin C-fragment compete to bind to a limited fixed concentration of tetanus antibody. The immunoassay technique described in this work shows promise as a component of an integrated microfluidic device amenable to automation and relevant to development of clinical diagnostic devices.

Tetanus neurotoxin is produced by the anaerobic bacterium *Clostridium tetani* and is one of the most toxic substances known.[1] It binds to nerve cells, penetrates the cytosol, and blocks neurotransmitter release causing spastic paralysis. Vaccination has proven to be the most-effective intervention for protection of human populations from tetanus and other infectious agents. Efficacy of vaccines against tetanus can be determined objectively by measuring the concentration of antibodies in serum.[2,3] Conventional immunoassays such as enzyme-linked immunosorbent assays (ELISA) are commonly used to measure concentrations of toxins in clinical samples or to assess antibody response to vaccination.[2,4,5] A typical ELISA is performed using a solid surface to immobilize one of the components (antibody or antigen) with multiple subsequent incubation and washing steps to separate the bound from unbound species. These assays typically require long assay times (hours) and appreciable amounts of sample and reagents (e.g., requiring both a primary and a secondary antibody).[2]

Over the past decade, microfluidic-based analytical devices incorporating electrophoresis have dramatically impacted the field of analytical chemistry by speeding analysis while using smaller sample and reagent volumes.[6−9] Electrophoresis in a capillary format has been demonstrated as an efficient means to separate immune complex from free antibody or antigen.[10−13] In such systems, immune complex and analyte are separated based upon charge-to-mass differences. A complete description of electrophoretic immunoassay advances may be found in recent reviews and references therein.[14,15] In addition to eliminating solid-phase associated problems regarding antigen immobilization, specific advantages of microdevice-based electrophoretic immunoassays include the potential for shortened incubation times (as compared to solid-phase systems), simplified assay protocols as compared to the multiple wash and detection steps required for conventional immunodiagnostics such as ELISA, use of a single antibody (as compared to matched pairs generally required for ELISA), and clean baselines yielding easily interpreted electropherograms. As microdevice form factors are amenable to system integration and automation, several groups have demonstrated microdevices as

* To whom correspondence should be addressed. E-mail: aeherr@sandia.gov.
† Now at Stanford University, Stanford, CA 94305.

(1) Lightstone, F. C.; Prieto, M. C.; Singh, A. K.; Piqueras, M. C.; Whittal, R. M.; Knapp, M. S.; Balhorn, R.; Roe, D. C. *Chem. Res. Toxicol.* **2000**, *13*, 356−362.
(2) Pickering, J. W.; Martins, T. B.; Schroder, M. C.; Hill, H. R. *Clin. Diagn. Lab. Immunol.* **2002**, *9*, 872−876.
(3) Gergen, P.; McQuillan, G. M.; Kiely, M.; Ezzatirice, T. M.; Sutter, R. W.; Virella, G. *N. Engl. J. Med.* **1995**, *23*, 761−766.
(4) Simonsen, O.; Bentzon, M. W.; Heron, I. *J. Biol. Stand.* **1986**, *14*, 231−239.
(5) Schauer, U.; Stemberg, F.; Rieger, C. H. L.; Buttner, W.; Borte, M.; Schubert, S.; Mollers, H.; Riedel, F.; Herz, U.; Renz, H.; Herzog, W. *Clin. Diagn. Lab. Immunol.* **2003**, *10*, 202−207.
(6) Harrison, D. J.; Fluri, K.; Seiler, K.; Fan, Z. H.; Effenhauser, C. S.; Manz, A. *Science* **1993**, *261*, 895−897.
(7) Effenhauser, C. S.; Manz, A.; Widmer, H. M. *Anal. Chem.* **1993**, *65*, 2637−2642.
(8) Jacobson, S. C.; Hergenroder, R.; Koutny, L. B.; Ramsey, J. M. *Anal. Chem.* **1994**, *66*, 1114−1118.
(9) Woolley, A. T.; Mathies, R. A. *Anal. Chem.* **1995**, *67*, 3676−3680.
(10) Nielsen, R. G.; Rickard, E. C.; Santa, P. F.; Sharknas, D. A.; Sittampalam, G. S. *J. Chromatogr.* **1991**, 177−185.
(11) Schultz, N. M.; Kennedy, R. T. *Anal. Chem.* **1993**, *1*, 3161−3165.
(12) Shimura, K.; Karger, B. L. *Anal. Chem.* **1994**, *66*, 9−15.
(13) Schmalzing, D.; Nashabeh, W.; Yao, X. W.; Mhatre, R.; Regnier, F. E.; Afeyan, N. B.; Fuchs, M. *Anal. Chem.* **1995**, *67*, 606−612.
(14) Shimura, K.; Zhi, W.; Matsumoto, H.; Kasai, K. *Anal. Chem.* **2000**, *72*, 4747−4757.
(15) Yeung, W. S. B.; Luo, G. A.; Wang, Q. G.; Ou, J. P. *J. Chromatogr., B* **2003**, *797*, 212−228.

10.1021/ac0489768 CCC: $30.25
Published on Web 12/03/2004

an elegant architecture for conducting integrated immunoassays.[16−19] Such demonstrations hold promise for development of automated, high-throughput systems for medical diagnostics.[20]

Attaining adequate species discrimination with electrophoresis-based immunoassays can be challenging. Large analytes such as antibodies and immune complexes vary little in charge-to-mass characteristics.[15] Techniques such as sodium dodecyl sulfate−polyacrylamide gel electrophoresis (SDS−PAGE) allow excellent discrimination of species by size, but SDS can disrupt fragile immune complexes, making quantitation of complexes impossible. Nondenaturing PAGE techniques, both with and without detergent, have been shown to retain the biological activity necessary for intact immune complexes yet allow analyte discrimination.[21,22] The ability to discriminate among antigen, antibody, and immune complexes based upon size, as well as charge-to-mass ratio, mitigates the sometimes poor resolution observed using nonsieving electrophoretic immunoassay techniques.

Recently, photopolymerized sieving structures have been shown to perform favorably for on-chip DNA sizing,[23] DNA and protein localization,[24−28] chromatography,[29−31] and protein sizing.[32−34] In this work, we report on on-chip electrophoretic immunoassays for rapid and sensitive detection of anti-tetanus toxin and tetanus toxin C-fragment levels in buffer and spiked serum samples. The on-chip immunoassays employ a native PAGE separation in lithographically photopatterned cross-linked sieving gels for detection and quantification of tetanus antibody and toxin levels. Use of in situ fabricated polymer matrixes in microfluidic devices could further aid development of chip-based immunoassays.[16,17,19]

EXPERIMENTAL SECTION

Chemicals. Recombinant tetanus toxin C-fragment (TTC, the atoxic binding portion of the native tetanus toxin,[35] supplier reported molecular weight, MW 50 000) and monoclonal anti-tetanus toxin C-fragment (anti-TTC) were purchased from Roche (Indianapolis, IN). Fluorescein isothiocyanate (FITC) labeled bovine serum albumin (BSA*, MW 66 000) was purchased from Sigma (St. Louis, MO). Green fluorescent protein (GFP, MW 27 000) was purchased from Qbiogene (Montréal, Canada). Bovine serum was obtained from Sigma and centrifuged at 6000 rpm for 20 min prior to use. The water-soluble photoinitiators 2,2′-azobis-(2-methylpropionamide) dihydrochloride (V-50) and 2,2′-azobis-[2-methyl-*N*-(2-hydroxyethyl)propionamide] (VA-086) were purchased from Wako Chemicals (Richmond, VA). Solutions of 3-(trimethoxysilyl)propyl methacrylate (98%), 40% acrylamide, and 30% (37.5:1) acrylamide/bisacrylamide were purchased from Sigma. Premixed 10× Tris-glycine (25 mM Tris, pH 8.3, 192 mM glycine) electrophoresis buffer was purchased from BioRad (Hercules, CA). Deionized water (18.2 MΩ) was obtained using an Ultrapure water system from Millipore (Milford, MA).

FITC and Alexa Fluor 488 (Molecular Probes, Eugene, OR) were used to fluorescently label TTC using protocols found in the product literature (MP 00143). FITC was used for CCD imaging experiments, while Alexa Fluor 488 was used in single-point detection experiments. Fluorescently labeled TTC is herein generically referred to as TTC*. FITC was abandoned in favor of Alexa Fluor 488, as FITC was found to dissociate from the labeled proteins, thus resulting in variable fluorescent signals from the internal standard and the analyte. The final concentrations of TTC* stock solutions were measured using an absorbance method outlined by Molecular Probes (MP 06434, product insert for F-6434).

Chip Fabrication. The microchips were fabricated from Schott D263 glass wafers (4-in. diameter, 1.1-mm thickness; S. I. Howard Glass Co., Worcester, MA) using standard photolithography, wet etching, and bonding techniques as described previously.[31] The chips contained offset double-T junctions. Separation channels were either 6.1 or 6.7 cm in length, depending on the device used. The injection arms and buffer arm measured 0.5 cm in length. The channels were 40 μm deep and 100 μm wide. To form buffer reservoirs, Nanoport assemblies from Upchurch Scientific (Oak Harbor, WA) were attached via holes in the cover plate using thermally cured adhesive rings.

The microchannels were conditioned prior to polyacrylamide gel polymerization following a procedure similar to that described by Kirby et al.[36] Using this two-step procedure, microchannels were functionalized using acrylate-terminated self-assembled monolayers and subsequently coated with linear polyacrylamide. Exact details of the coating procedure were previously reported in Herr and Singh[34] and are summarized here. After initial channel cleaning with 1 M NaOH (10-min flush), water (10-min flush), and a final air purge, channels were conditioned with a 2:3:5 mixture of 3-(trimethoxysilyl)propyl methacrylate, glacial acetic acid, and deionized water for 30 min. Note that the conditioning mixture was vigorously agitated during mixing (especially during addition of the water) and thoroughly degassed and sonicated for 5 min. At the end of the 30-min conditioning step, the channels were purged with air and subsequently rinsed with deionized water for 10 min. To form the linear polyacrylamide channel

(16) Chiem, N.; Harrison, D. J. *Anal. Chem.* **1997**, *69*, 373−378.
(17) Koutny, L. B.; Schmalzing, D.; Taylor, T. A.; Fuchs, M. *Anal. Chem.* **1996**, *68*, 18−22.
(18) Qiu, C. X.; Harrison, D. J. *Electrophoresis* **2001**, *22*, 3949−3958.
(19) Cheng, S. B.; Skinner, C. D.; Taylor, J.; Attiya, S.; Lee, W. E.; Picelli, G.; Harrison, D. J. *Anal. Chem.* **2001**, *73*, 1472−1479.
(20) Kricka, L. J. *J. Clin. Ligand Assay* **2002**, *25*, 317−324.
(21) Ou, J. P.; Wang, Q. G.; Cheung, T. M.; Chan, S. T. H.; Yeung, W. S. B. *J. Chromatogr., B* **1999**, *727*, 63−71.
(22) Schagger, H.; Vonjagow, G. *Anal. Biochem.* **1991**, *199*, 223−231.
(23) Brahmasandra, S. N.; Ugaz, V. M.; Burke, D. T.; Mastrangelo, C. H.; Burns, M. A. *Electrophoresis* **2001**, *22*, 300−311.
(24) Timofeev, E. N.; Kochetkova, S. V.; Mirzabekov, A. D.; Florentiev, V. L. *Nucleic Acids Res.* **1996**, *15*, 3142−3148.
(25) Guschin, D.; Yershov, G.; Zaslavsky, A.; Gemmell, A.; Shick, V.; Proudnikov, D.; Arenkov, P.; Mirzabekov, A. *Anal. Biochem.* **1997**, *1*, 203−211.
(26) Proudnikov, D.; Timofeev, E.; Mirzabekov, A. *Anal. Biochem.* **1998**, *15*, 34−41.
(27) Vasiliskov, A. V.; Timofeev, E. N.; Surzhikov, S. A.; Drobyshev, A. L.; Shick, V. V.; Mirzabekov, A. D. *Biotechniques* **1999**, *27*, 592−606.
(28) Olsen, K. G.; Ross, D. J.; Tarlov, M. J. *Anal. Chem.* **2002**, *15*, 1436−1441.
(29) Yu, C.; Svec, F.; Frechet, J. M. J. *Abstr. Am. Chem. Soc.* **2000**, *26*, U101−U101.
(30) Shediac, R.; Ngola, S. M.; Throckmorton, D. J.; Anex, D. S.; Shepodd, T. J.; Singh, A. K. *J. Chromatogr., A* **2001**, *925*, 251−263.
(31) Throckmorton, D. J.; Shepodd, T. J.; Singh, A. K. *Anal. Chem.* **2002**, *74*, 784−789.
(32) Han, J. Y.; Singh, A. K. *J. Chromatogr., A* **2004**, *1049*, 204−209.
(33) Shediac, R.; Pizarro, S. A.; Herr, A. E.; Singh, A. K. *Proceedings of the uTAS 2003 Symposium*, Squaw Valley, CA, October 5−9, 2003; Transducers Research Foundation, 2003; pp 971−974.
(34) Herr, A. E.; Singh, A. K. *Anal. Chem* **2004**, *76*, 4727−4733.
(35) Helting, T. B.; Zwisler, O. *J. Biol. Chem.* **1977**, *252*, 187−193.
(36) Kirby, B. J.; Wheeler, A. R.; Zare, R. N.; Fruetel, J. A.; Shepodd, T. J. *Lab Chip* **2003**, *3*, 5−10.

coating, channels were flushed with a solution of 5% (w/v) acrylamide containing 5 mg/mL V-50 and exposed to a 100-W mercury lamp for 10 min. After the coating treatment, chips were flushed with deionized water for 5 min and stored hydrated and refrigerated at 5 °C.

To achieve the desired total acrylamide gel concentration (T), T% polyacrylamide gel matrixes were fabricated by adjusting the volume of the 30% acrylamide/bisacrylamide solution with native Tris−glycine run buffer. (Safety consideration: the acrylamide used to fabricate the sieving gel is a neurotoxin absorbed through the skin. Users should consult the appropriate MSDS for proper safety precautions.) The final monomer and cross-linker solution contained 0.2% (w/v) VA-086 photoinitiator. In a manner similar to other studies,[33,34] pressure-driven flow was used to fill all channels with the polyacrylamide gel solution. Briefly, both thorough degassing of the polyacrylamide gel solution and a low flow rate channel-filling protocol were essential to obtain high-quality polymerized gels. The chip was then exposed to a 4-W UV illumination source at $\lambda = 365$ nm for 15−20 min. The UV photopatterning apparatus was shielded to protect the experimenter from stray UV light.

Apparatus. Platinum electrodes were inserted at each fluid reservoir to provide electrical connectivity to a programmable high-voltage power supply developed and fabricated in-house. Separations were conducted using the standard double T-chip in a manner consistent with conventional microdevice operation.[34] A typical voltage program was as follows: during sample loading, 300 V/cm was applied between the sample and sample waste reservoirs for 240 s; separations were initiated by applying a positive high voltage at buffer waste and grounding the buffer reservoir. No "pull-back" voltage[37] was necessary during injection, as the high viscosity of the polymer matrix reduced leakage of sample from the loading arms into the separation channel.

Species transport was observed using epifluorescence microscopy techniques and digital imaging, as described elsewhere;[34] while laser-induced fluorescence (LIF) and single-point detection were used to obtain electropherograms and sensitivity data. Briefly, the CCD imaging system employed epifluorescence microscopy in conjunction with a 1300 × 1030, Peltier-cooled interline CCD camera (CoolSnap HQ, Roper Scientific, Trenton NJ). A 0.31× demagnifier (Diagnostic Instruments Inc., Sterling Heights, MI) was used to increase the field of view projected onto the CCD. In the LIF system, excitation light (argon ion laser, 488 nm) was frequency modulated using a mechanical chopper (220-Hz modulation) and reflected off of a dichroic mirror (XF2010) through a 40× microscope objective (New Focus, Inc, San Jose, CA) that defined the detection point on the microchip. A custom fixture mounted on a three-axis translation stage allowed for focusing and alignment of the laser beam with respect to the separation channel. Fluorescence was filtered spectrally (535-nm notch filter, XF3084) and spatially (iris) before detection by a Hamamatsu H5784 photomultiplier tube (PMT). The signal from the PMT was demodulated using a lock-in amplifier (Stanford Research Systems, Sunnyvale, CA), and signal was collected using a computer via a data acquisition interface (6020E DAQPad, National Instruments, Austin, TX). Data were collected using an in-house program written in LabVIEW (National Instruments).

Chip-Based Native PAGE Immunoassays. Direct PAGE Immunoassay Sample. TTC* and anti-TTC samples were prepared in a 1× native Tris−glycine buffer, as well as in a diluted bovine serum solution. To perform direct immunoassays for anti-TTC, the initial concentration of TTC* was constant among samples and the volume of anti-TTC was varied within the groups to obtain the desired concentration of antibody in the final sample. All samples were adjusted to a final volume of 50 μL through addition of 1× native Tris−glycine buffer (or bovine serum). Samples were mixed by gentle aspiration using a pipet and incubated, shielded from light, in plastic tubes at room temperature for at least 1 h. To avoid protein denaturation and breakdown of antibodies into heavy and light chains, the immunoassays were conducted without boiling or inclusion of SDS in the sample.[38,39]

Competitive PAGE Immunoassay Sample. Sample solutions consisting of TTC*, TTC, and anti-TTC were prepared in 1× native Tris−glycine buffer off-chip. The molar ratio of TTC* to anti-TTC, as well as the final sample volume, was kept constant for all competitive samples. The concentration of unlabeled TTC added to the sample solutions was varied to obtain the desired final unlabeled TTC concentration. In all cases, the anti-TTC was the final component added to the competitive sample solutions. Incubation conditions were as described for the direct immunoassays.

Immunoassay Quantitation. For use in generating direct dose−response curves, peak areas were calculated by estimating (using Simpson's rule) the area of each peak in the electropherograms acquired by the LIF instrument. The peak area corresponding to the immune complex was normalized by the peak area of the free dye internal standard. During both the competitive and direct experiments, the amount of free TTC* initially present in each sample mixture was constant, as was the amount of internal standard present. Peak height was used to generate the competitive dose−response curve, as the complex peak was difficult to accurately define with respect to the background signal. In the competitive case, peak height was normalized to the maximum free dye peak height for each run. Normalization was used to correct for variation in the injected sample volume, as well as for any uncorrected variations in excitation illumination.

RESULTS AND DISCUSSION

Polyacrylamide Gel Characterization. To characterize the native PAGE performance of the in situ photopolymerized polyacrylamide gels, apparent mobility information was collected for three model proteins (BSA*, GFP, TTC*) at various polyacrylamide gel concentrations and applied electric field strengths using the CCD imaging system. Mobilities were calculated from the known applied field strength, the measured frame-to-frame displacement of each species, and the time between frames. No obvious dependence of apparent mobility of TTC* on field strength was observed for field strengths ranging from 245 to 410 V/cm. Additionally, BSA*, GFP, and TTC* showed a linear dependence between peak motion and time for all field strengths (245−410

(37) Ermakov, S. V.; Jacobson, S. C.; Ramsey, J. M. *Anal. Chem.* **2000**, *72*, 3512−3517.

(38) Thorne, J. M.; Goetzinger, W. K.; Chen, A. B.; Moorhouse, K. G.; Karger, B. L. *J. Chromatogr., A* **1996**, *744*, 155−165.

(39) Ou, J. P.; Chan, S. T. H.; Yeung, W. S. B. *J. Chromatogr., B* **1999**, *731*, 389−394.

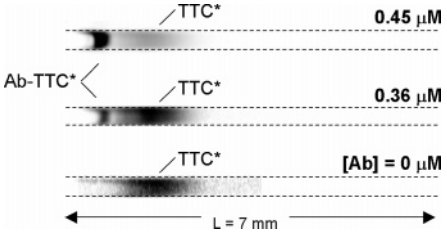

Figure 1. CCD images of a PAGE immunoassay after an elapsed separation time of 16 s. Inverted gray scale images are shown for decreasing amount of anti-TTC present in the sample. The initial concentration of TTC* was constant in each sample mixture (0.5 μM), while the concentration of anti-TTC was varied. Sample injection occurred to the left and adjacent to each imaged area shown. Separation conditions: 6% gel; E = 350 V/cm. The image aspect ratio has been adjusted for clarity.

V/cm) and gel porosities (4, 6, 10%) considered (n = 27; $R^2 \geq$ 0.982). All three protein species exhibited a marked decrease in apparent mobility as polyacrylamide concentration increased. The observed trend indicates that the separation mechanism consists of both an electrophoretic component and a sieving component. Ferguson analysis can be employed to relate the polyacrylamide gel concentration to the measured apparent mobility of a protein through the retardation coefficient, K_r.[40,41] A plot of $\ln(\mu)$ versus polyacrylamide concentration yields K_r. The K_r values reported by Gonenne and Lebowitz.,[42] for similar size native proteins, agree within 25%.

Separation resolution, SR, for an internal standard (free FITC dye) and TTC* was employed to further characterize the native PAGE behavior of 4 and 6% acrylamide gels at a range of applied electric field strengths (E = 245−410 V/cm). Using the relation SR = $\Delta L/4\sigma_{av}$, where ΔL is the peak-to-peak distance and σ_{av} is the average width (standard deviation) of the two concentration distributions, SR was calculated by a least-squares Gaussian fit to image data (axial intensity distributions) at a set elapsed separation time (Δt_{sep} = 5 s). Over the range of electric field strengths investigated, SR showed a linear proportionality to $\sqrt{E}$ for both the 4 (SR = $0.45\sqrt{E} - 5.8$, $R^2 = 0.98$) and 6% gels (SR = $0.16\sqrt{E} - 1.4$, $R^2 = 0.90$). SR was markedly higher in the 6% acrylamide gel as compared to the 4% acrylamide gel for all E investigated, as expected. Observed mobility and SR dependence on polyacrylamide concentration indicates that the gel characteristics can be readily tailored to satisfy assay resolution requirements.

On-Chip Direct Immunoassay for Anti-TTC. Figure 1 presents CCD images of chip-based direct immunoassays using a 6% polyacrylamide gel after an elapsed separation time of 16 s. In each sample, TTC* was used as the fluorescently labeled antigen and anti-TTC was used as the analyte. Detection of a second peak, having a lower apparent mobility than the mobility of free TTC*, indicates formation of a fluorescent immune complex (Ab-TTC*); as the relative magnitudes of the TTC* and Ab-TTC* complex peaks are directly related to the antibody concentration. As the amount of unlabeled anti-TTC is increased, the intensity of the TTC* band decreases with a concomitant intensity increase in the immune complex band.

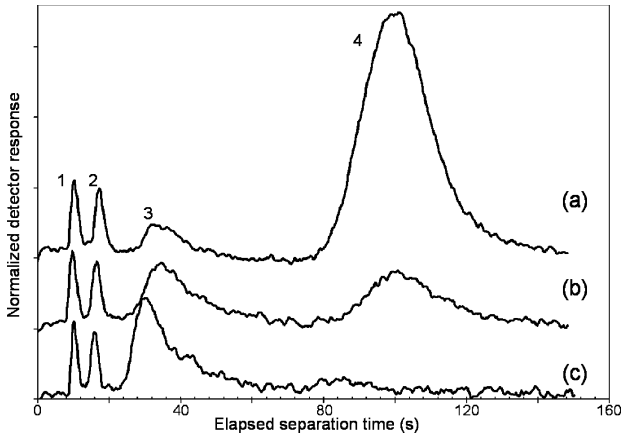

Figure 2. Single-point detection of a direct PAGE immunoassay. Electropherograms of a direct immunoassay containing a constant TTC* concentration of 13.0 nM with decreasing anti-TTC concentration values of (a) 5.4, (b) 1.4, and (c) 0.2 nM. Peaks 1 and 2 correspond to free dye and were used as a standard, peak 3 is the free TTC*, and peak 4 is the fluorescent immune complex. Detector response was normalized to the internal standard for each case. E = 300 V/cm, total length 6.1 cm, and length to detector 6 mm.

The PAGE immunoassays presented in this work have separation times that are competitive with reported on-chip free solution electrophoresis-based immunoassays. As shown using full-field imaging in Figure 1, the immune complex is nearly resolved from the free TTC* in less than 16 s and in a 7-mm-long separation distance. CZE-based immunoassays have been reported to complete in 2−3 min with Fab and in 13 min with whole antibody.[11] On-chip free solution electrophoresis immunoassays have been reported to complete in less than 40 s.[16]

Quantitation of peak height and peak area was employed to generate dose−response curves for the tetanus system. Single-point detection yielded electropherograms for the native PAGE immunoassay of low-concentration TTC* samples, as presented in Figure 2. In agreement with the CCD images shown in Figure 1, the peak associated with the immune complex is clearly observable as the amount of anti-TTC is increased. Separation of the immune complex from free TTC* is complete within 150 s, using single-point detection. Figure 3 shows the dose−response curve for the measurement of anti-TTC by direct immunoassay. In these experiments, the TTC* concentration was held constant at 13 nM, while the concentration of anti-TTC was varied. The data in Figure 3 were fit using a four-parameter logistic model of the form

$$F = \beta_2 + \frac{(\beta_1 - \beta_2)}{1 + ([\mathrm{Ab}]/\beta_3)^{\beta_4}}$$

where F and [Ab] are the normalized peak area and anti-TTC concentration, respectively. β_1 is the asymptote as [Ab] $\rightarrow 0$, β_2 is the asymptote as [Ab] $\rightarrow \infty$, β_3 is the logarithm of the predicted peak area at the response midpoint (halfway between the two peak area asymptotes), and β_4 is the Hill coefficient, which is related to the steepness of the sigmoidal dose−response curve. In this case, the best nonlinear least-squares fit to the data was obtained using the parameter values: $\beta_1 = 0.04$, $\beta_2 = 1.0$, $\beta_3 = 3.5 \times 10^{-9}$, and $\beta_4 = 1.9$.

(40) Ferguson, K. A. *Metabolism* **1964**, *13*, 985.
(41) Rodbard, D.; Chrambach, A. *Proc. Natl. Acad. Sci. U.S.A.* **1970**, *65*, 970−977.
(42) Gonenne, A.; Lebowitz, J. *Anal. Biochem.* **1975**, *64*, 414−424.

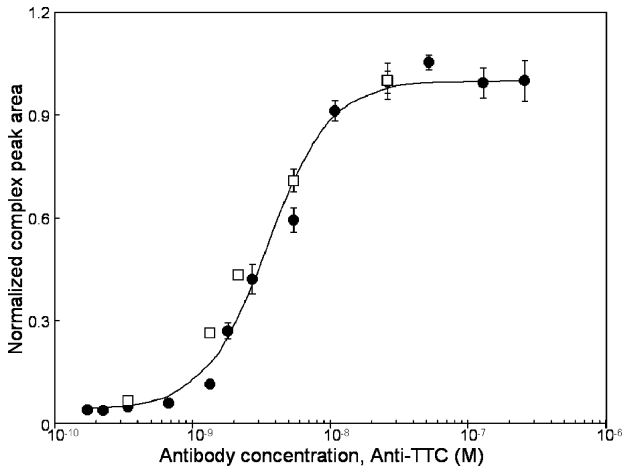

Figure 3. Dose−response curve for anti-TTC by PAGE immunoassay. Solid symbols correspond to the peak area of the Ab-TTC* complex normalized by the peak area of internal standard in a buffer system. Four-parameter logistic equation was used to fit the data. Open symbols correspond to normalized peak area as described, but in diluted bovine serum. Error bars indicate the standard error associated with each mean normalized peak area (n = 4−5).

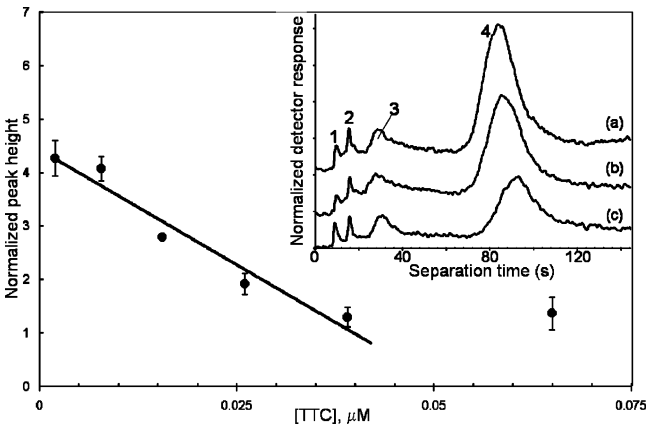

Figure 4. Dose−response curve for TTC by competitive PAGE immunoassay. Solid symbols correspond to the peak height of the Ab-TTC* complex normalized by the peak height of the free dye. The linear fit through the points indicated has a correlation coefficient of 0.95. Error bars indicate standard error in the measurements (n = 3−5). (Inset) Electropherograms for constant concentrations of TTC* (13.0 nM) and anti-TTC (6.0 nM) with TTC concentrations of (a) 2.0, (b) 7.8, and (c) 15.6 nM. Peaks 1 and 2 correspond to free dye (peak 2 used as standard), peak 3 is the free TTC*, and peak 4 is the complex. Detector response was normalized to the internal standard for each case. E = 300 V/cm, total length 6.1 cm, and length to detector 6 mm.

The effects of interfering substances on the ability of the immunoassay to accurately determine the quantity of tetanus antibody in biological specimens was determined by measuring the normalized peak areas for direct anti-TTC immunoassays conducted in a 1/100 diluted bovine serum specimen containing 13 nM TTC*. Figure 3 shows the normalized peak area measurements from the adulterated specimen in comparison to the results from the buffer-based immunoassay. Peak areas for both the buffer and serum immunoassays were normalized to the β_2 value for each dose−response curve. The peak area measurements from the serum sample can be described by the same four-parameter model used to generate the dose−response curve obtained in buffer solutions. Electropherograms and subsequent fluorometric analysis indicate a greater amount of total fluorescence from samples in serum versus samples in Tris−glycine buffer solutions.

The minimum detectable concentration (MDC) was defined as the lowest concentration of analyte that resulted in a response (fluorescence signal) three standard deviations higher than the response at zero concentration. For the LIF/PMT system described, this corresponds to a MDC of 680 pM unlabeled anti-TTC. Conventional immunoassay methods (e.g., ELISA) have reported detection limits in the pico- to nanomolar range,[43] indicating that the present microscale system performs well.

On-Chip Competitive Immunoassay for TTC. In addition to direct immunoassays, competitive format immunoassays for tetanus toxin C-fragment were performed in the photopatterned cross-linked gels. As conducted, the competitive immunoassays were designed to use TTC* as a fluorescent reporter antigen and TTC as analyte, both of which compete to form complexes with the anti-TTC. Figure 4 shows the dose−response curve for the competitive immunoassay. The inset in Figure 4 shows representative electropherograms from a competitive immunoassay having constant concentrations of TTC* (13 nM) and anti-TTC (6 nM) and varied TTC concentrations. Competitive immunoassays rely upon competition between fluorescently labeled antigen and unlabeled sample antigen to form an immune complex with the unlabeled antibody (or antibody fragment). Quantitation of either the labeled antigen peak or fluorescent immune complex peak should, ideally, allow determination of the amount of unlabeled antigen present in a given sample. As is observable in the inset to Figure 4, the fluorescent complex peak (peak 4) height diminishes as TTC is added to the sample with a concomitant increase in the peak height of the free TTC* (peak 3). These observations are indicative of expected competitive immunoassay behavior; wherein an increase in sample antigen concentration results in both an increase in observed free labeled antigen and a decrease in the observed fluorescent immune complex, as the sample antigen−antibody immune complex is not fluorescent. Eventually, as the concentration of TTC is increased in Figure 4, nonlinearity is observed in the dose−response curve and is presumably indicative of saturation of the anti-TTC with TTC.

Polyacrylamide Gel Structures. UV photopatterned polymers allow localization of the sieving matrix with high spatial resolution. As microdevice-based analyses mature, increased device functionality and sophistication necessitates the ability to selectively optimize and functionalize regions of an analytical microdevice for specific transport and separation mechanisms. Such spatial patterning enables extended device functionality.[25,28,31] Figure 5 shows an image of a microdevice with selective patterning of a polyacrylamide gel structure. Confinement of polyacrylamide gel to a single channel (the separation channel in the standard offset double-T device shown in Figure 5) offers key advantages when conducting either SDS or native PAGE analysis of a sample mixture. Nevertheless, the presence of polymer matrix in all channels of the device resulted in improved device performance for the immunoassays presented in this work. In systems with cross-linked polymer localized in the separation channel only,

(43) Diamandis, E. P.; Christopoulos, T. K.; Khosravi, M. J. In *Immunoassay*; Diamandis, E. P., Christopoulos, T. K., Eds.: Academic Press: San Diego, 1996.

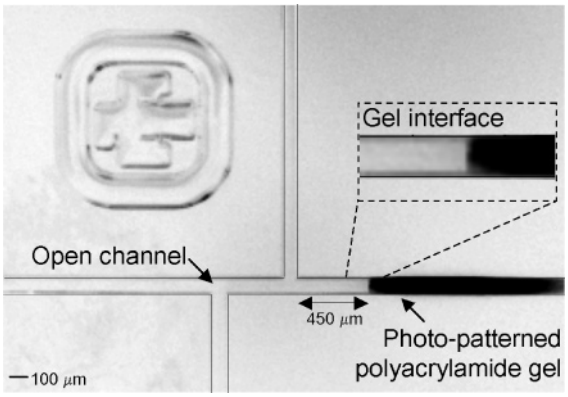

Figure 5. In situ photopolymerized polyacrylamide gels. Image of glass microchip with cross-linked polyacrylamide gel localized in the separation channel. Normally visually undetectable, the gel contains dye that appears black in this inverted gray scale image. The inset shows the open channel/gel interface. For clarity, microchannel sidewalls have been enhanced.

interaction of large species (i.e., immune complexes) with the gel interface resulted in extensive sieving and exclusion of the large species from the separation channel. The observed sieving behavior is attributed to a "skin" effect at the polymer/liquid interface; in which an interfacial layer having smaller pores than the bulk cross-linked polyacrylamide is formed. In this work, PAGE analyses of both free and immune complexed species were of interest; thus, all data presented were obtained from systems with polyacrylamide gel fabricated uniformly in all channels. We are actively exploring large-species interaction with the cross-linked polymer/free solution interface.

The polyacrylamide gels proved to be durable under limited current, limited field strength operation. Several individual chips were successfully used for hundreds of separations (each separation lasting 5−7 min), when the current flow was limited to ~10 μA and applied field strengths were limited to ~410 V/cm. The mode of polymer failure has not been fully characterized. In agreement with published reports of in situ polymerized gel structure failure modes,[28] a drop in the electrical resistance of the gel-filled microchannel correlated well with gel failure. In the gels presented in this work, failure manifested itself through the formation of visible voids in the bulk of the polymer. Nevertheless, several chips (>15) were successfully employed for hundreds of hours of native PAGE immunoassays over several months of use. High gel structure and device yields (>90%) make the devices potentially attractive as a disposable diagnostic platform useful in clinical analysis of patient samples.

(44) Chiem, N. H.; Harrison, D. J. *Clin. Chem.* **1998**, *44*, 591−598.

CONCLUSIONS

Native PAGE separations of proteins and tetanus immune complexes have been demonstrated in an in situ photopatterned separation medium of cross-linked polyacrylamide gels. A dose−response curve for the direct immunoassay for antibodies to tetanus toxin C-fragment was generated and showed limiting behaviors expected of conventional direct immunoassays, as quantified through a four-parameter logistic model. Further, direct immunoassays for antibodies to tetanus performed in a diluted serum solution also agreed with trends anticipated from a conventional immunoassay format. The minimum detectable antibody concentration was measured to be 680 pM. The microsystem was extended to include a competitive immunoassay for tetanus toxin C-fragment, which resulted in generation of an additional dose−response curve. Direct and competitive immunoassays were completed with separation times of less than 3 min.

The direct and competitive immunoassays reported illustrate the simplicity, speed, and quantitation associated with on-chip electrophoresis-based immunodiagnostics. We anticipate several possible improvements to the immunoassay. For example, combining the assay with on-chip mixing and metering,[44] extension of the system to include multianalyte detection in a parallel separation format, and enhanced automation will enable high-throughput analysis of complex samples devoid of user intervention.

ACKNOWLEDGMENT

The authors thank J.S. Brennan, G.B. Sartor, S.L. Jamison, W.H. Kleist, R.F. Renzi, and J.F. Stamps for their assistance. This work was supported by the National Institute of Dental and Craniofacial Research (Grant U01DE014961). Sandia is a multiprogram laboratory operated by Sandia Corp., a Lockheed Martin Co., for the United States Department of Energy under Contract DE-AC04-94AL85000.

Received for review July 13, 2004. Accepted October 14, 2004.

AC0489768